Materials Science & Engineering A 645 (2015) 20–27

Contents lists available at ScienceDirect

Materials Science & Engineering A

journal homepage: www.elsevier.com/locate/msea

Beneficial influence of an intercritically rolled recovered ferritic matrix on the mechanical properties of TRIP-assisted multiphase steels

S. Godet [a], P.J. Jacques [b,*]

[a] Université Libre de Bruxelles, 4MAT (Materials Engineering, Characterization, Synthesis and Recycling), Avenue F.D. Roosevelt 50, 1050 Brussels, Belgium
[b] Université catholique de Louvain, Institut de Mécanique, Matériaux et Génie Civil (iMMC), IMAP, Place Sainte Barbe 2, B-1348 Louvain-la-Neuve, Belgium

ARTICLE INFO

Article history:
Received 30 July 2014
Received in revised form
26 July 2015
Accepted 27 July 2015
Available online 29 July 2015

Keywords:
Steel
Thermomechanical processing
EBSD
Phase transformation
Dislocations
Mechanical characterisation

ABSTRACT

The present study deals with the microstructure and mechanical properties of intercritically rolled TRIP-assisted multiphase steels. It is shown that the occurrence of the TRIP effect in a recovered ferritic matrix brings about an improved strength–ductility balance with respect to a fully recrystallised ferrite matrix. On the other hand, the intercritical deformation does not influence the austenite transformation rate during straining at room temperature. The improvement of the mechanical properties results from the interactions between the transformation strain and the recovered ferrite.

1. Introduction

TRIP-assisted multiphase steels constitute now a well established class of high strength steels [1]. They consist of carbide-free bainite and retained austenite embedded in a ferritic matrix. The formation of such a microstructure requires different steps during the processing route [2]. The first one consists of the formation of a mixture of intercritical ferrite and austenite, while during the second one austenite partially transforms to bainite. During this bainite transformation, carbon diffuses from the supersaturated ferrite platelets into the surrounding austenite [3]. As carbide precipitation is hindered by the relatively large silicon (or aluminium) content (1–2 wt%) of this type of alloy, the austenite is enriched with carbon throughout bainitic holding and can finally be retained after quenching to room temperature [4].

Numerous studies scrutinised the role of several processing parameters or the effect of the microstructure on the mechanical properties. Much attention was devoted to the understanding of the formation of this kind of microstructure and of the resulting mechanical properties in the case of cold rolled and intercritically annealed steels [5–10]. On the other hand, several studies considered the processing of TRIP-aided multiphase steels by thermomechanical processing. However, most of these studies dealt with deformation stages above the no-recrystallisation temperature (T_{nr}) of austenite or considered the role of micro-alloying elements [11–17]. Hardly anything has been reported in the case of intercritical rolling of low carbon TRIP-aided steels [18]. In the case of ferritic steels, if the warm rolling practice was developed since it leads to an effective compromise between cost savings (due to lower reheating temperature) and mechanical performances [19], it is well known that the recovered ferrite that is induced presents a higher strength but completely depleted strain hardening capabilities [20]. It is also worth noting that some specific results were recently reported in the case of the δ-TRIP steels that present a ferrite–austenite microstructure at all temperature due to their specific chemical composition [21], or in the case of medium-Mn steels [22].

The aim of this study is to demonstrate the beneficial influence of an intercritical rolling stage on the mechanical properties of low alloy TRIP-assisted multiphase steels. Contrarily to the well known detrimental influence of a non-recrystallised ferrite state on its work hardening capabilities, the activation during straining of the martensitic transformation of retained austenite grains embedded in a recovered ferrite matrix brings about improved levels of strength and ductility. This paper thus deals with (i) the effect of hot deformation in the intercritical temperature range on the microstructure development and (ii) the relationship between the hot rolling parameters and the resulting mechanical properties.

* Corresponding author.
E-mail address: pascal.jacques@uclouvain.be (P.J. Jacques).

http://dx.doi.org/10.1016/j.msea.2015.07.082
0921-5093/

Table 1
Chemical composition of the investigated steel.

Element	C	Si	Mn	P	S	Al
wt%	0.15	1.52	1.49	0.015	0.009	0.032

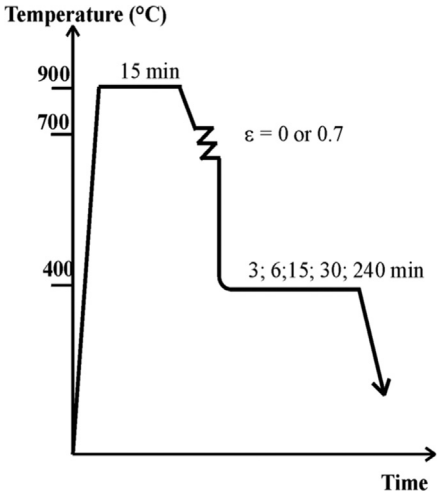

Fig. 1. Schematic representation of the thermomechanical processing route.

2. Experimental procedure

The composition of the investigated steel is given in Table 1. Its composition is typical of high silicon TRIP-assisted multiphase steels, i.e. a low-carbon steel with a significant amount of silicon (that enables the austenite to be retained at room temperature by incomplete bainite transformation), and some manganese (that provides hardenability). No micro-alloying elements were added. The steel was provided as two 150 kg ingots from which 100 mm thick plates were first hot-rolled down to 20 mm. These 20 mm thick plates were used as the raw material. The no-recrystallisation temperature (T_{nr}) as well as the Ar_3 temperature were estimated by hot torsion owing to the evolution of the mean flow stress during continuous cooling conditions similar to the thermomechanical process described below. Temperatures of 920 °C and 770 °C were found for T_{nr} and Ar_3, respectively.

The thermomechanical process (TMP) was simulated considering two steps. The first step (roughing) aimed at homogenising the microstructure and reducing the grain size owing to the austenite recrystallisation. After reheating at 1250 °C for 45 min, two deformation passes starting at 900 °C were applied for a total deformation of 1. The specimens were then quenched in boiling water (which provides a constant cooling rate of ~50 °C s^{-1}) down to 650 °C, held at this temperature for 1 h and finally furnace cooled as a normalising treatment. The second stage, which is depicted in Fig. 1, aimed at generating the multiphase microstructures. The specimens were reheated at 900 °C for 15 min. They were allowed to air cool down to 700 °C where they were deformed to a true strain of 0.7. This deformation temperature lies in the austenite/ferrite domain. For the sake of comparison, some specimens were not deformed at 700 °C. The different specimens were then quenched in a salt bath at 400 °C for the bainite transformation stage. Bainitic holding times of 3, 6, 15, 30 min and 4 h were investigated. The specimens were finally water quenched to room temperature. Amongst these different bainitic holding times, 30 min revealed to bring about the best strength–ductility balance while 4 h of holding leads to the complete decomposition of austenite into bainitic ferrite and carbides

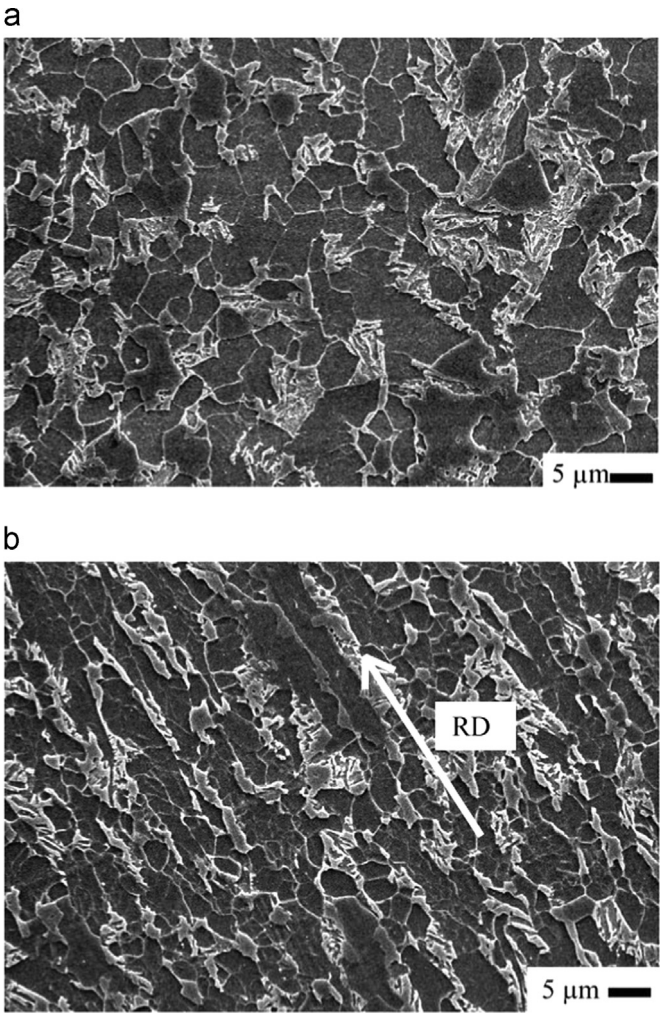

Fig. 2. SEM micrograph of the microstructure of (a) the specimen not deformed at 700 °C and (b) the specimen deformed to ε=0.7 at 700 °C. Both specimens were then held for 30 min at 400 °C.

[2,23]. In what follows, the different specimens will be denoted MPXXYY (MP for 'multiphase'), where XX will correspond to the intercritical deformation and YY to the bainitic holding time.

The mechanical properties were measured in uniaxial tension with the tensile axis oriented in the rolling direction on samples machined following the European standard EN10002-1. The initial gauge length and width were 50 and 12.5 mm, respectively. The cross-head speed was 2 mm min^{-1}. Measured loads and elongations (with an extensometer) were converted to true stresses and true strains. Five samples were measured for each condition. Standard deviations for stress and strain are of the order of 10 MPa and 0.02, respectively. Strain hardening was described using the incremental strain hardening exponent (n_{incr}) defined as

$$n_{incr} = \frac{d\ln\sigma}{d\ln\varepsilon} \quad (1)$$

Microstructures were studied by SEM after conventional Nital etching. A prior 2 h annealing at 200 °C allowed the martensite and austenite to be distinguished [24]. Some specimens were also characterised by EBSD [25]. They were first ground and subsequently polished with diamond paste down to 1 μm. The last step consisted of a 1 h polishing stage with a 0.05 μm colloidal silica solution. Different areas were scanned with adequate step sizes in order to distinguish the features of the finely grained microstructures.

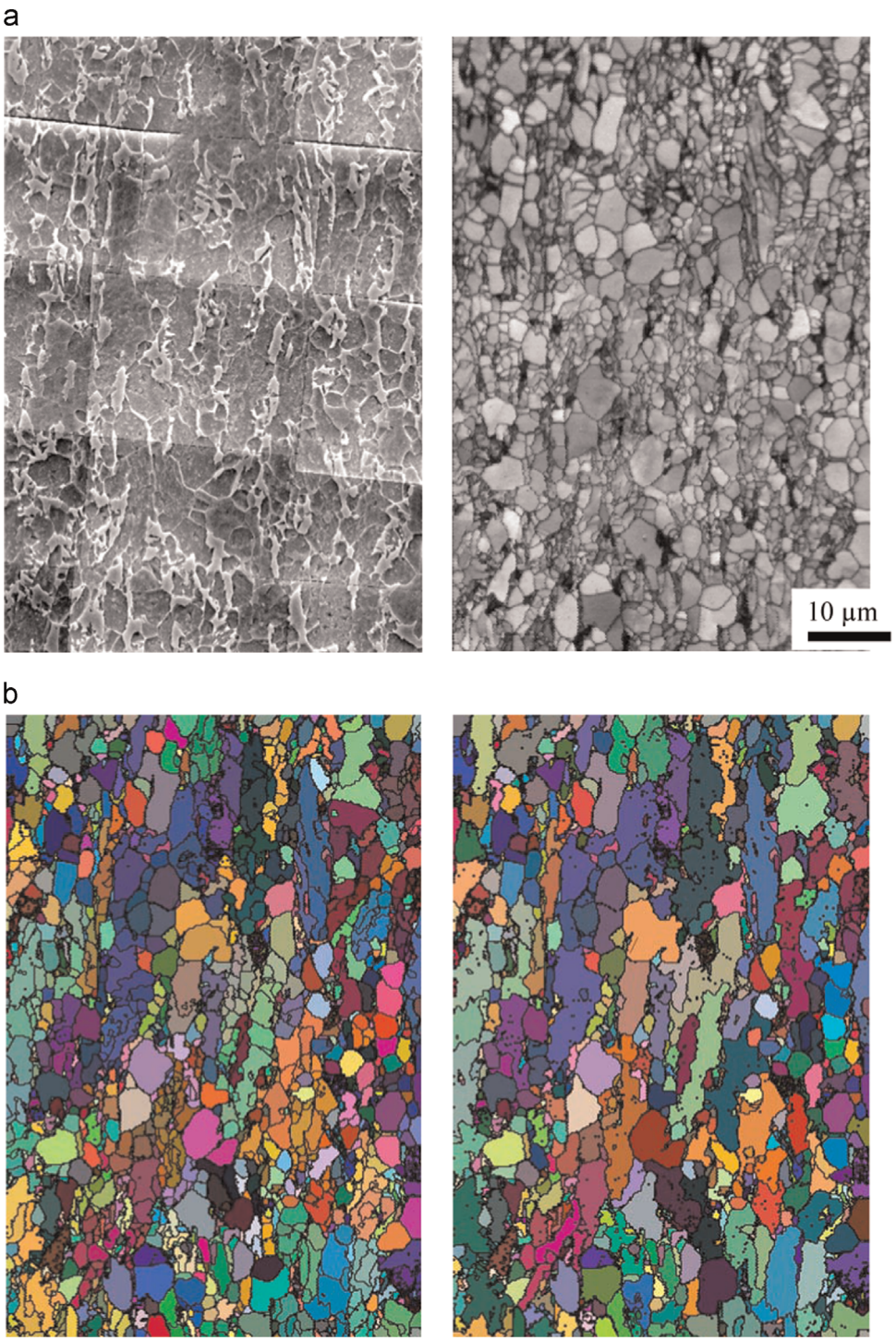

Fig. 3. SEM and EBSD maps of the same zone of specimen MP0730 intercritically rolled to ε=0.7 at 700 °C and transformed at 400 °C for 30 min. (a) SEM micrograph; (b) EBSD band contrast map; (c) and (d) maps of reconstructed grains with boundaries corresponding to misorientations of 5° or 15°, respectively (Rodrigues space colour coding). (For interpretation of the references to color in this figure legend, the reader is referred to the web version of this article.)

The evolution of the retained austenite volume fraction during straining was measured by neutron diffraction on 1 cm^3 rotating specimens. For comparison, austenite volume fractions were also measured on some of the samples by Mössbauer spectroscopy and by X-Ray diffraction (Co K$\alpha_{1,2}$ radiation) with a rotating sample holder to avoid texture effects. The proportion of intercritical ferrite was determined by image analysis on Dual Phase ferrite–martensite specimens. Finally, the proportion of bainitic ferrite was calculated as the balance fraction, assuming the absence of martensite in the initial microstructure.

3. Results and discussion

Fig. 2 compares the microstructure of specimens either not deformed (MP0030) or strained to 0.7 at 700 °C (MP0730) and held for 30 min at 400 °C. Specimen MP0030 presents the typical microstructure of TRIP-assisted multiphase steels, i.e. a ferritic matrix with a dispersion of bainite–austenite grains. It is also worth noting that the ferrite grains are equiaxed. In the case of specimen MP0730, there is a clear alignment of the microstructure along the rolling direction while the same phases, i.e. ferrite,

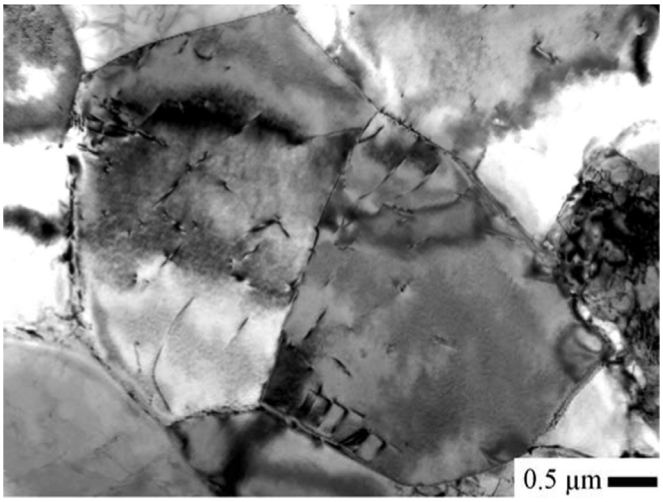

Fig. 4. TEM micrograph showing the recovered structure of the ferritic matrix of the intercritically rolled specimen.

bainite and retained austenite, are present. It is worth noting that some equiaxed grains can also be found in the matrix of specimen MP0730 due to the formation of strain-induced ferrite [26].

Fig. 3 presents SEM and EBSD micrographs of the same area of the microstructure of specimen MP0730. The alignment along the rolling direction is clearly visible on the SEM micrograph but almost completely absent on the band contrast map (Fig. 3(b)). On this figure, the microstructure is shown to be constituted of very fine equiaxed grains and of some larger dislocation-free grains. The very small grains are not revealed by nital etching. Fig. 3 (c) and (d) present reconstructed grains considering misorientations for the boundaries of 5° and 15°, respectively. These maps suggest that the small ferrite grains of Fig. 3(b) actually result from extensive recovery.

This last point is confirmed by the TEM micrograph of Fig. 4 that reveals that the small grains of ferrite are in fact subgrains delineated by arrangements of dislocations. It thus proves that ferrite dynamically recovers during deformation so that the elongated grains actually contain slightly misoriented subgrains. Recovery is indeed the principal softening mechanism for a phase like ferrite with high stacking fault energy [27]. It was also found that these subgrains are present in specimens directly quenched after deformation [17], confirming that they were formed during deformation (dynamic recovery). The ferritic matrix of specimen MP0730 also contains some dislocation-free grains. These were either formed at the end of the deformation stage or during the transfer to the salt bath. Their low dislocation densities and their high angle boundaries lead to rapid growth in the deformed ferritic matrix [28].

Fig. 5 compares the general morphology of bainite-retained austenite aggregates resulting from the partial bainite transformation of intercritical austenite in the case of samples MP0030 and MP0730. Fig. 5(a) and (d) correspond to EBSD band contrast maps illustrating the general morphology of the microstructure. Fig. 5(b) and (e) on the one hand and 5(c) and 5(f) on the other hand correspond to the inverse pole figure maps of the face centred cubic (austenite) and body centred cubic (ferrite+bainitic ferrite) phases, respectively. In both cases, the contour of a particular prior austenite grain has been drawn owing to the identical crystallographic orientation of the remaining austenite islands as well as the general morphology revealed by the SEM micrographs of Fig. 2. Fig. 5(e) shows that the retained austenite presents gradients of orientation, confirming the no-recrystallisation state of this phase. Furthermore, these EBSD maps clearly show that the intercritical rolling stage does not modify the general morphology and arrangement of the retained austenite+bainite aggregates present in these TRIP-aided steels. Particularly, the grain size of both phases is of the same order for both processing conditions.

The proportion of the different phases constituting the specimens MP0030 and MP0730 are given in Table 2. The intercritical rolling does not seem to influence the amount of retained austenite. These specimens mainly differ by their proportion of ferrite with the amount which is induced by the intercritical rolling in the case of specimen MP0730.

The influence of the intercritical deformation on the flow curves is illustrated in Fig. 6 for bainitic holding times of 30 min and 4 h, respectively. The comparison of the yield strength of these curves clearly shows that (i) the intercritical deformation leads to an increase of the yield strength of more than 100 MPa; (ii) a 4 h bainitic holding stage leads to an increase of the yield strength of 60–70 MPa with respect to a 30 min bainitic hold. The strengthening due to the intercritical rolling results from the deformation and recovery of the different phases. The increase due to the longer bainitic stage may be due to the carbides precipitation resulting from the austenite decomposition at the end of the bainitic holding [2,23].

The influence of the intercritical deformation on the levels of tensile strength and uniform elongation also strongly depends on the bainitic holding time. Indeed, Fig. 7 shows that the intercritical deformation brings about an improvement of both strength and uniform elongation when austenite is retained through a partial bainite transformation (up to 30 min of holding) while the tensile strength increases but the uniform elongation decreases in the case of a complete bainite transformation (4 h of holding). The improvement of the mechanical properties when a TRIP effect is activated was not anticipated since it is well known that recovered microstructures exhibit deteriorated work hardening capabilities [29]. On the contrary, the detrimental influence of the hot deformation without recrystallisation fits with previously observed behaviour. Indeed, recovered ferrite in IF steels has been shown to display lower work-hardening capabilities than recrystallised ferrite [29]. Some improvement relying on the bainitic ferrite formed from deformed austenite (sometimes called ausformed bainite) cannot be argued here. Indeed, bainite in TRIP-aided multiphase steels is a carbide-free bainite that already presents a specific morphology of fine and parallel platelets [2]. As shown on Fig. 5, intercritical rolling does not modify the morphology of this specific bainite, only its density of dislocations as for intercritical ferrite.

The difference in tensile properties induced by intercritical deformation can also be illustrated by comparing the evolution of the incremental work-hardening exponent with plastic straining, as depicted in Fig. 8. As already demonstrated previously [1,2,5,6], the beneficial influence of the TRIP effect is demonstrated when comparing specimens MP0030 and MP004h. After 5% of plastic strain, the work-hardening rate of specimen MP004h starts decreasing whereas the occurrence of the TRIP effect in specimen MP0030 leads to an increase in the work-hardening exponent. It means that the work-hardening capabilities of the bainite/ferrite matrix start exhausting while the TRIP effect acts as the major work-hardening source.

More curiously, intercritical rolling can also lead to some improvement of the work hardening rate when a TRIP effect is activated. In the case of a microstructure without retained austenite, the work hardening rate of intercritically rolled microstructure is lower than without this hot deformation stage as illustrated by the curves of specimens MP074h and MP004h, respectively. On the contrary, intercritical rolling improves the work hardening rate when a TRIP effect is activated as illustrated by the curves of specimens MP0730 and MP0030.

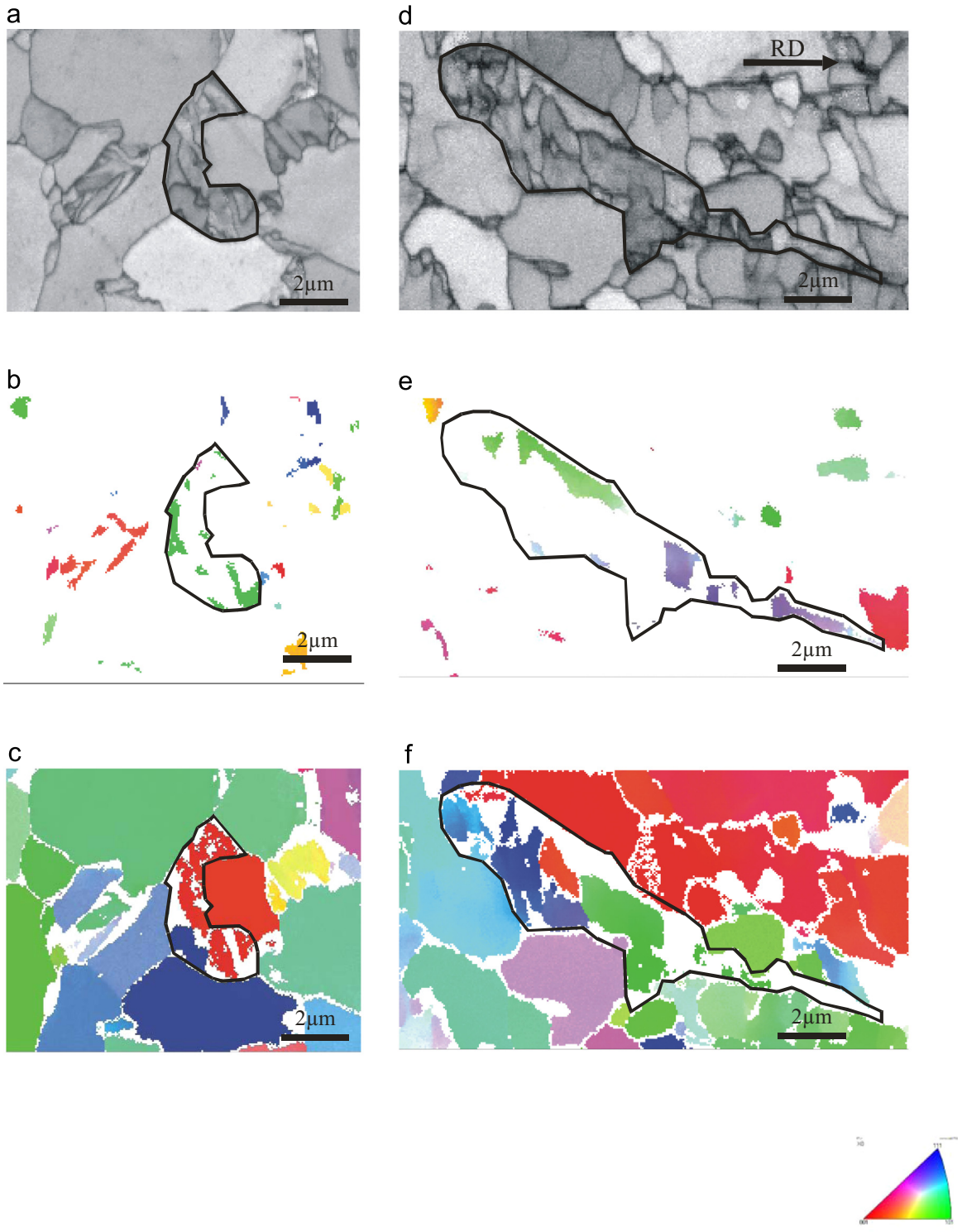

Fig. 5. EBSD maps of specimens MP0030 (a–c) and MP0730 (d–f) illustrating the morphology of the retained austenite–bainitic ferrite aggregates as a function of the intercritical rolling conditions. (a) and (d) correspond to EBSD band contrast maps, (b) and (e) on the one hand and (c) and (f) on the other hand correspond to the inverse pole figure maps of the face centred cubic (austenite) and body centred cubic (ferrite+bainitic ferrite) phases, respectively.

Table 2
Proportions of the different phases present in the specimens either not deformed or rolled to $\varepsilon=0.7$.

	α (%)	α_b (%)	γ_r (%)
MP0030	54 ($\pm$3)	37	9.2 ($\pm$0.4)
MP0730	62 ($\pm$3)	28	9.6 ($\pm$0.4)

When the TRIP effect is activated during straining, it was shown that the retained austenite parameters mostly affecting the work hardening rate are the initial amount of retained austenite and the austenite transformation rate during straining [1,2,10]. The evolution of the retained austenite volume fraction during plastic straining is shown in Fig. 9 for these two specimens. As already shown in Table 2, they both display comparable initial volume fractions of retained austenite before tensile testing.

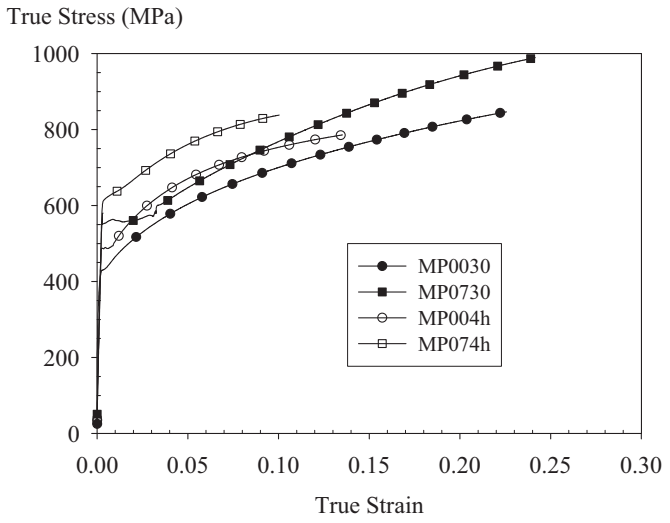

Fig. 6. True stress–true strain curves of specimens that were not deformed at 700 °C or deformed to a true strain of $\varepsilon=0.7$ and held for bainitic holding times of 30 min and 4 h at 400 °C, respectively.

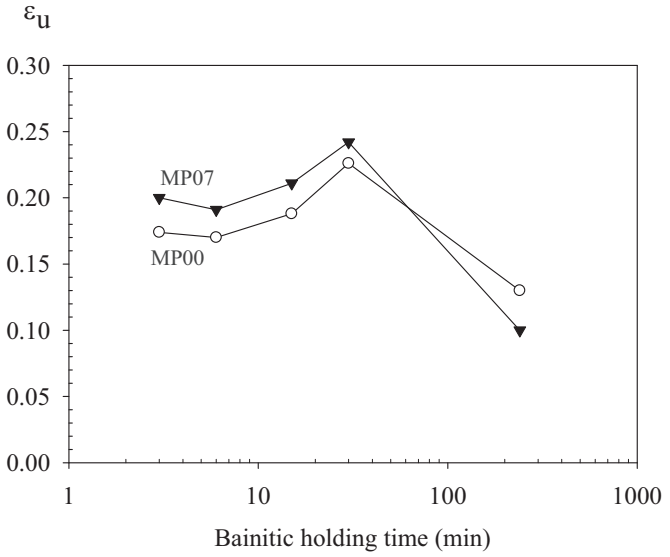

Fig. 7. Evolution of the uniform elongation as a function of the bainitic holding time for samples intercritically deformed (MP07) or undeformed (MP00).

Furthermore, they present comparable transformation rates and final amounts of retained austenite at necking. There is no detectable difference in the transformation rate during deformation. It can thus be concluded that while the intercritical rolling does not influence the strain-induced transformation of austenite into martensite at room temperature, it improves the 'efficiency' of the TRIP effect, i.e. the increase of work hardening for a given amount of transforming austenite.

As it was clearly demonstrated [1,2,9], the improvement of the work hardening rate by the TRIP effect relies on 2 phenomena: (i) the formation of the martensite which is harder than the austenite (a dynamic composite effect); (ii) the local plastic straining of the ferritic phases surrounding the transforming grains of austenite that brings an extra source of dislocations. It could be first argued that the larger work-hardening rate can be attributed to the creation of a harder martensite that inherits the deformed state of the austenite so that it sustains a larger load. The yield strength and tensile strength of the different specimens are summarised in Table 3. The consequences of the work-hardening

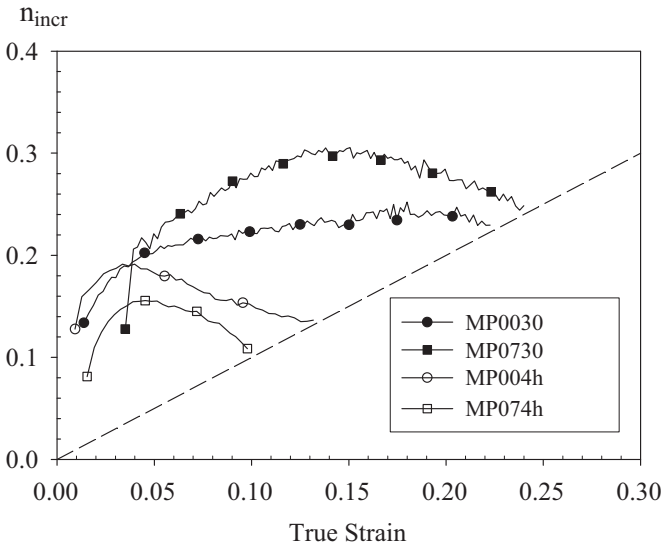

Fig. 8. Evolution of the incremental work-hardening exponent of specimens that were not deformed at 700 °C or deformed to a true strain of $\varepsilon=0.7$ and held for 30 min or 4 h at 400 °C, respectively.

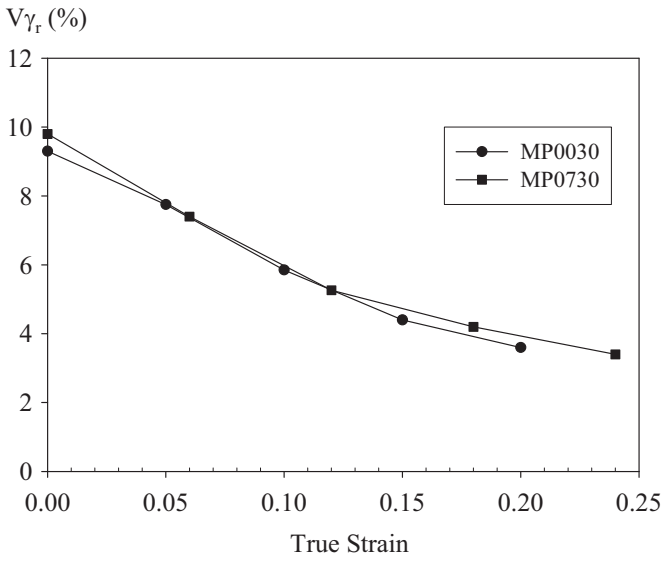

Fig. 9. Evolution of the retained austenite volume fraction of specimens held for 30 min at 400 °C.

Table 3
Yield strength and tensile strength of the different specimens.

	Yield strength (MPa) (YS)	Tensile strength (MPa) (TS)	TS–YS (MPa)
MP0030	436	846	410
MP0730	550	989	439
MP004h	490	785	295
MP074h	619	838	219

behaviour can be expressed as the difference between the tensile strength and the yield strength. The TRIP effect in a recovered ferrite/bainite matrix (MP0730) brings about 28 MPa of additional work-hardening when compared to specimen MP0030, whereas in the absence of the TRIP effect, the recovered ferrite/bainite matrix (MP074h) causes a drop of 76 MPa when compared to specimen MP004h. If the 28 MPa extra hardening was only due to a harder martensite that constitutes only 7% of the global microstructure, it

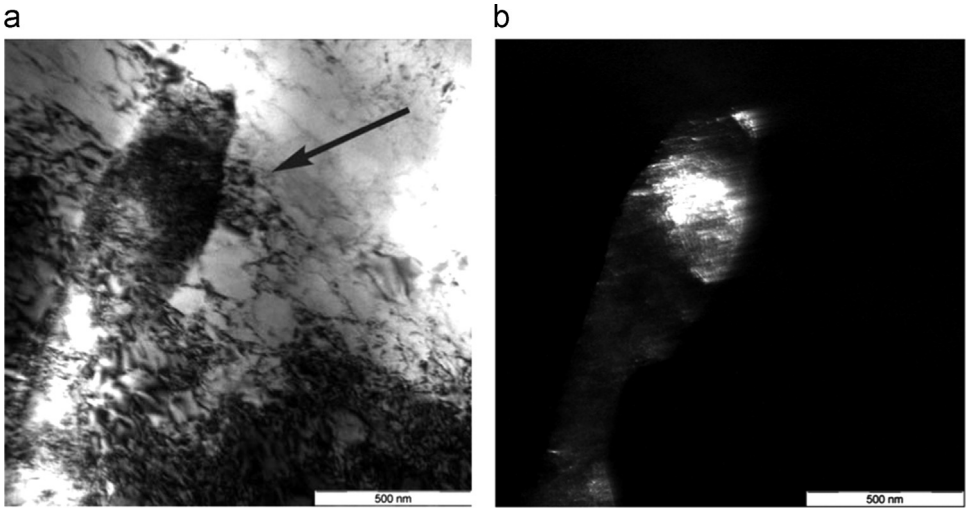

Fig. 10. (a) Bright field TEM micrograph illustrating the dislocations generated within the recovered ferrite along a martensite grain (confirmed by dark field micrograph of (b)) resulting from transformed retained austenite (specimen MP0730).

would mean that the strength level of the martensite is increased by more than 500 MPa. Moreover, if the 76 MPa drop in hardening of the ferrite/bainite matrix is taken into account, the martensite strength of specimen MP0730 should be about 1500 MPa higher than in specimen MP0030. This is of the order of the reported yield strength of martensite [30–33] and is thus very doubtful. Moreover, it is impossible for a dispersed hard phase to sustain a load which is 4 to 5 times larger than the stress sustained by the matrix. Indeed, debonding or other damage mechanisms would take place and unload the hard phase. If there is a raise in the martensite strength, this cannot account for the totality of the increase in the work-hardening capabilities.

The improvement in the work-hardening properties is also related to the plastic straining of the ferritic phase. Indeed, beside the formation of a hard phase, it is known that the martensitic transformation is accompanied by a transformation strain that causes the plastic deformation of the surrounding ferrite grains [1,2,11,34]. The martensitic transformation acts as an extra source of dislocations that increases the work-hardening of the ferritic matrix and thus influences in a large way the work-hardening behaviour of the composite microstructure. Fig. 10 presents TEM micrographs of specimen MP0730 uniaxially strained to 0.05 at room temperature. As demonstrated for Dual Phase and cold rolled and annealed TRIP-assisted multiphase steels [1,2], these bright field and dark field micrographs show that a large density of dislocations is present in the ferrite grain adjacent to a martensite grain that appeared within the transforming retained austenite. It is proposed that the dislocations generated in the recovered ferritic matrix by the martensitic transformation interact with the dislocations priorly generated by rolling in the grain interior or with the dislocation walls of the subgrain boundaries. The TRIP effect thus acts as a dislocation source external to the ferrite, still active even when the intrinsic sources of the deformed ferrite are exhausted. The interactions of this external source with the recovered arrangements of dislocations improve the work-hardening capabilities so that recovered ferrite work-hardens in a larger way than a recrystallised ferrite. However, in the absence of an external source of free dislocations, the recovered ferritic matrix is unable to generate new free dislocations and its work-hardening properties are very much decreased when compared to the recrystallised matrix.

4. Conclusion

This study aimed at characterising and understanding the effect of a deformation applied during intercritical annealing on the microstructure and mechanical properties of TRIP-assisted multiphase steels. Contrarily to ferritic steels, it is shown that this intercritical deformation improves the work hardening rate, and thus the strength–ductility balance, of multiphase microstructures exhibiting a TRIP effect. This enhancement of the mechanical properties by intercritical deformation results from the interaction between (i) the recovered structure of the intercritically deformed ferritic matrix in which there is a starvation of the intrinsic dislocation sources and (ii) the supplementary dislocations generated within the ferrite surrounding the austenite grains that transform to martensite in order to accommodate the transformation strains.

Acknowledgements

The authors acknowledge the financial support from the Interuniversity Attraction Poles Program from the Belgian State through the Belgian Policy Agency; Contract IAP7/21 “INTEMATE”. PJJ acknowledges the FRS–FNRS.

References

[1] P.J. Jacques, Q. Furnemont, F. Lani, T. Pardoen, F. Delannay, Acta Mater. 55 (2007) 3681–3693.
[2] P.J. Jacques, Curr. Opin. Solid State Mater. Sci. 8 (2004) 259–265.
[3] H.K.D.H. Bhadeshia, J.W. Christian, Metall. Trans. A 21 (1990) 767–797.
[4] H.K.D.H. Bhadeshia, D.V. Edmonds, Met. Sci. 17 (1983) 411–419.
[5] M. De Meyer, D. Vanderschueren, B.C. De Cooman, ISIJ Int. 39 (1999) 813–822.
[6] E. Girault, P. Jacques, P. Ratchev, J. Van Humbeeck, B. Verlinden, E. Aernoudt, Mater. Sci. Eng. A 273–275 (1999) 471–474.
[7] E. Girault, A. Mertens, P. Jacques, Y. Houbaert, B. Verlinden, J. Van Humbeeck, Scr. Mater. 44 (2001) 885–892.
[8] P. Jacques, X. Cornet, Ph Harlet, J. Ladrière, F. Delannay, Metall. Mater. Trans. 29 (1998) 2383–2393.
[9] P.J. Jacques, E. Girault, Ph Harlet, F. Delannay, ISIJ Int. 41 (2001) 1061–1067.
[10] P.J. Jacques, J. Ladrière, F. Delannay, Metall. Mater. Trans. 32 (2001) 2759–2768.
[11] M. Delince, Y. Bréchet, J.D. Embury, M.G.D. Geers, P.J. Jacques, T. Pardoen, Acta Mater. 55 (2007) 2337–2350.
[12] S.J. Kim, C.G. Lee, T.H. Lee, S. Lee, ISIJ Int. 40 (2000) 692–698.
[13] E.V. Pereloma, I.B. Timokhina, P.D. Hodgson, Mater. Sci. Eng. A 273 (1999) 448–452.
[14] D.S. Liu, M. Militzer, W.J. Poole, Metall. Mater. Trans. A 38 (2007) 894–909.
[15] S. Hashimoto, S. Ikeda, K. Sugimoto, S. Miyake, ISIJ Int. 44 (2004) 1590–1598.

[16] H.J. Jun, S.H. Park, S.D. Choi, C.G. Park, Mater. Sci. Eng. A 379 (2004) 204–209.
[17] S. Godet, P. Harlet, F. Delannay, P.J. Jacques, Steel Res. 73 (2002) 280–286.
[18] A. Bodin, J. Sietsma, S. Van Der Zwaag, Metall. Mater. Trans. A 33 (2002) 1589–1603.
[19] M.R. Barnett, J.J. Jonas, ISIJ Int. 39 (1999) 856–873.
[20] D.L. Bourell, O.D. Sherby, Metall. Trans. A 12 (1981) 140–142.
[21] H.L. Yi, K.Y. Lee, H.K.D.H. Bhadeshia, Mater. Sci. Technol. 27 (2011) 525–529.
[22] R. Zhang, W.Q. Cao, Z.J. Peng, J. Shi, H. Dong, C.X. Huang, Mater. Sci. Eng. A 583 (2013) 84–88.
[23] L. Zhao, T.A. Kop, V. Rolin, J. Sietsma, A. Mertens, P.J. Jacques, S. Van Der Zwaag, J. Mater. Sci. 37 (2002) 1585–1591.
[24] E. Girault, P. Jacques, P. Harlet, K. Mols, J. Van Humbeeck, E. Aernoudt, F. Delannay, Mater. Charact. 40 (1998) 111–118.
[25] S. Godet, J.C. Glez, Y. He, J.J. Jonas, P.J. Jacques, J. Appl. Crystallogr. 37 (2004) 417–425.
[26] P.D. Hodgson, A. Shokouhi, H. Beladi, ISIJ Int. 48 (2008) 1046–1049.
[27] F.J. Humphreys, M. Haterly, Recrystallisation and Related Annealing Phenomena, Pergamon Press, Oxford, 1996.
[28] A. Bodin, J. Sietsma, S. van der Zwaag, Mater. Charact. 47 (2001) 187–193.
[29] H. Réglé, in: G. Gottstein, D.A. Molodov (Eds.), Proceedings of the 1st Joint International Conference on Recrystallisation and Grain Growth, Springer Verlag, Aachen, 2001, pp. 695–699.
[30] G. Krauss, Metall. Mater. Trans. A 32 (2001) 205–221.
[31] M. Delince, P.J. Jacques, T. Pardoen, Acta Mater. 54 (2006) 3395–3404.
[32] P.J. Jacques, Q. Furnemont, S. Godet, F. Delannay, Philos. Mag. 86 (2006) 2371–2392.
[33] F. Lani, Q. Furnemont, T. Van Rompaey, F. Delannay, P.J. Jacques, T. Pardoen, Acta Mater. 55 (2007) 3695–3705.
[34] P. Jacques, Q. Furnémont, T. Pardoen, F. Delannay, Acta Metall. 49 (2001) 139–152.